
Desert Tortoise Occupancy Multi-year Multi-method Statistical Analysis

Final Report

Prepared for the:



desert conservation

PROGRAM

4701 W. Russell Rd.

Las Vegas, NV, 89118

Prepared by:

Biometrician on the Science Advisor Panel
for the Desert Conservation Program

Seth Harju

Heron Ecological, LLC

P.O. Box 235

Kingston, ID 83839



Heron Ecological, LLC

Introduction

In 2013, Clark County, Nevada's Desert Conservation Program (DCP) began implementing a 4+ year pilot study to investigate the utility of an occupancy monitoring program for monitoring desert tortoise (*Gopherus agassizii*) in the Boulder City Conservation Easement (BCCE; DCP 2011). Occupancy monitoring has been demonstrated as an efficient way to monitor desert tortoise populations (Zylstra et al. 2010). A key goal of this DCP study was to use the results to better understand spatial patterns of desert tortoise occurrence and to use those patterns to create a spatially-explicit predictive map of the probability of occurrence across the BCCE.

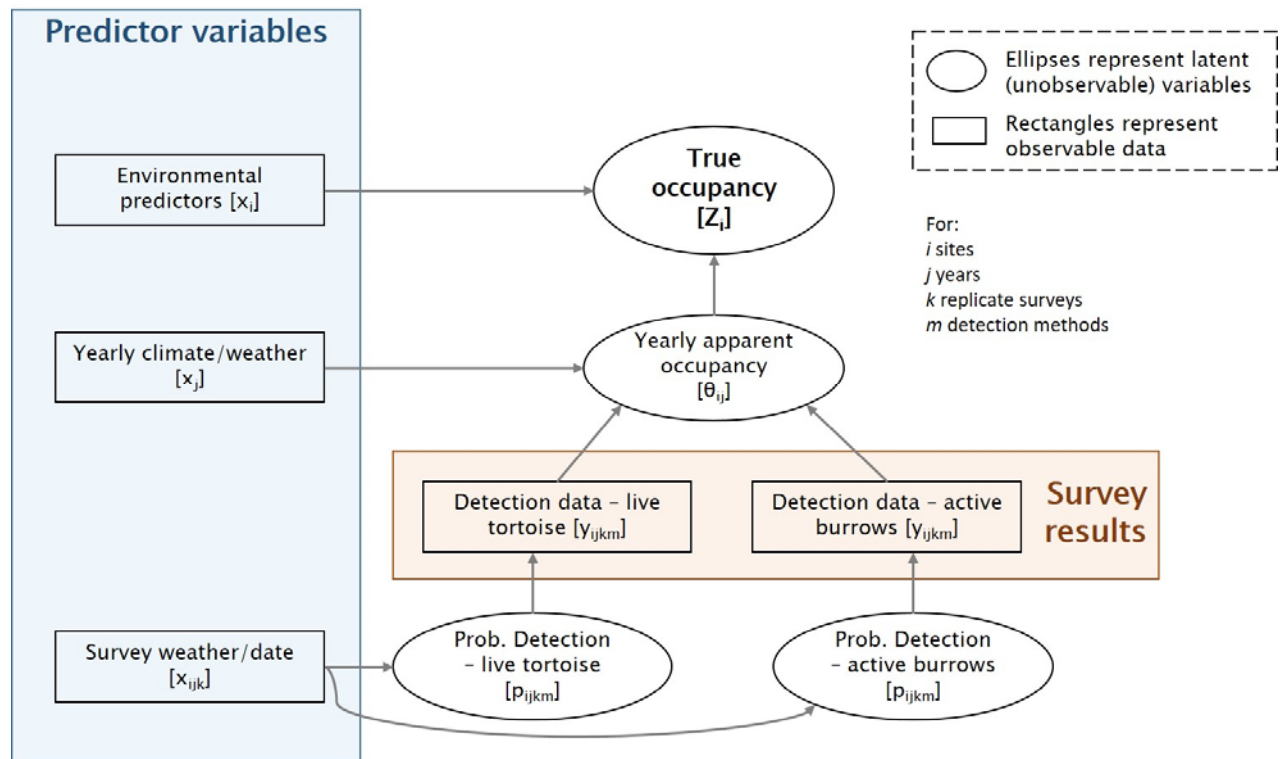
Occupancy surveys were initiated in spring 2013, with data collection through spring 2017 (to date). DCP (2011) provides full details on monitoring protocols for the study and data set described herein; a brief overview is presented here for clarity. Occupancy modeling (sensu MacKenzie et al. 2002) focuses on quantifying the probability that a sample site is occupied by a species given imperfect detection. When a species is surveyed for in the field, it is not always detected 100% of the time that it is present. Imperfect detection can potentially seriously underestimate the proportion of an area thought to be occupied by a species, leading to biased estimates of the range of species occurrence and biased estimates of relationships between species occurrence and environmental variables (MacKenzie et al. 2002). To remedy this, MacKenzie et al. (2002) developed a method involving multiple visits made to the same sample unit within a window in which the true occupancy state (either occupied or unoccupied) can be assumed constant (e.g., a season). The probability that a site was occupied given no detections can then be estimated. This modeling approach has been expanded to include a variety of increasingly complicated situations, including occupancy dynamics over multiple years, simultaneous occupancy patterns for multiple species, and defining occupancy as >2 mutually-exclusive 'states' (see Bailey et al. 2014 for recent review).

The ecology of desert tortoise presents several challenges for occupancy sampling. Desert tortoise occur at low population densities and can be both cryptic (when aboveground) or unavailable for detection (when belowground). Availability for detection can vary dramatically both within and among years in response to weather and vegetation conditions (Duda et al. 1999). In addition to variable detectability, desert tortoise home ranges can be larger than a feasible occupancy sample unit (e.g., mean minimum convex polygon home ranges of up to 16.2 ha; Franks et al. 2011). Maximum distances between consecutive telemetry relocations of over 5.3 km have been observed in the BCCE (DCP unpublished data). This means that for a sample unit, it is possible that it is 'occupied' during the season but a tortoise is not physically within the sample unit during a particular sampling event (i.e., "temporary emigration").

Standard occupancy models have been expanded to include both multiple methods of detection and surveying for a species at multiple scales (Nichols et al. 2008; Mordecai et al. 2011). Further, Royle & Kerry (2007) re-framed occupancy modeling as a Bayesian state-space model, which dramatically increases the flexibility of occupancy modeling beyond the original maximum likelihood framework. I modified the approaches of Nichols et al. (2008) and Mordecai et al. (2011) to address multiple temporal scales and to do so in a Bayesian state-space hierarchical model with two methods of desert tortoise detection, which can greatly improve precision of estimating occupancy parameters (Graves et al. 2012). There are three primary

levels to the hierarchy: the survey-level detection data, a year-specific apparent occupancy estimate, and an across-year true occupancy state. Figure 1 shows a conceptual representation of how environmental and weather predictors affect detection probabilities, observed detection data, yearly apparent occupancy, and latent true occupancy during the study period.

Figure 1. Conceptual model of desert tortoise occupancy in relation to environmental predictors on the Boulder City Conservation Easement, Clark County, Nevada, USA, 2013-2017. The primary focus of the analysis is on identifying the relationships between ‘environmental predictors’ and ‘true occupancy’ while accounting for all other model components.



The conceptual model highlights several important components of the analysis, starting from the bottom and working upwards. First, the probabilities of detecting live tortoises and active burrows are likely different and each is potentially influenced by observable factors, such as weather conditions and Julian date on the day of the survey. Second, observations of live tortoises and active burrows separately but jointly contribute to the estimate of whether a site *appears* occupied within that year. ‘Yearly apparent occupancy’ could also be termed ‘available for detection’ (sensu Mordecai et al. 2011) because we are making the assumption that true occupancy of a site is constant within the study period. Potential departures from this assumption are likely minimal based on desert tortoise life history (i.e., long-lived, low reproduction, long time to sexual maturity), results from preliminary analyses (i.e., juvenile desert tortoises were never encountered without an adult tortoise present), the ecological potential for confounding (i.e., dynamics confounded by prevailing weather and availability for

detection), and land management status (i.e., all sites are in a protected conservation easement and have been actively conserved since 1995). Yearly apparent occupancy can be considered separate samples of the true latent occupancy state. We note that in this study within each year, it is possible that temporary emigration is affecting the detection data, whereby within a year plots are occupied by a desert tortoise during one survey and not during another, which may be due to the tortoise temporarily emigrating from the plot. Because of this the occupancy estimates can be interpreted as the frequency of desert tortoise encounters rather than the proportion of sites occupied by the species (D. MacKenzie, *unpublished data*). This novel occupancy model allows us to explicitly estimate the relationships between landscape features and occupancy while simultaneously addressing variation in detectability (including probability of detection given presence, unavailability for detection given presence, and absence due to temporary emigration) both within and among years. Finally, the output from the model was used to build a predictive surface in a Geographic Information System (GIS) that delineates areas with different levels of relative probability of desert tortoise occurrence as a function of landscape variables. The predictive surface was then validated using two data sets to assess the robustness of the model outputs.

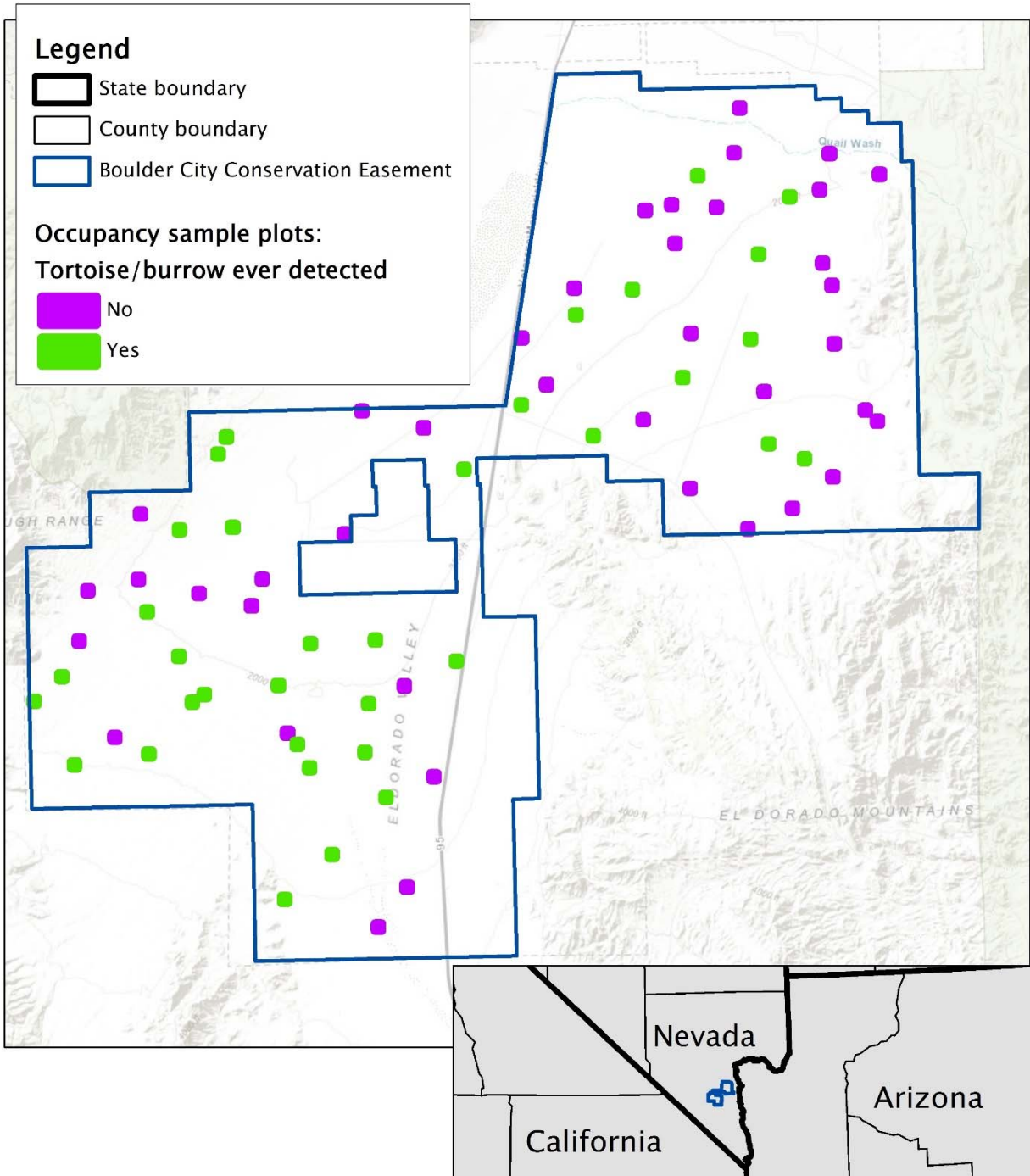
Methods

Field data collection

The field and remote-sensed environmental data were collected within the boundaries of the BCCE, Clark County, Nevada (Figure 2). The DCP leveraged the multiple-visit methodology at 80 sites in each year from 2013 – 2017, with the notable exception that the number of surveys at each site within a season increased from three to seven beginning in 2015 due to low detection probabilities. To compensate for cost increases, 20 sites were dropped from the project after 2014. Five of the 20 sites were dropped non-randomly (i.e., due to unique site geologies) and will be excluded from all analyses. The remaining 15 of 20 dropped sites were dropped at random, and are retained in the analyses (albeit only with data in 2013 and 2014). Thus the occupancy analysis data set consists of 75 sites, each with three independent desert tortoise presence surveys in 2013 and 2014, and a subset of 60 sites that each had seven independent desert tortoise presence surveys in 2015, 2016, and 2017.

DCP contractors also recorded two different types of indicators of the ‘presence’ of desert tortoise at a site: live tortoises and active burrows. Live tortoises are cryptic but mobile, whereas active burrows are static but uncommon. There are two parallel records in the detection data, one for live tortoises with a ‘1’ if a desert tortoise was observed during the survey and a ‘0’ if unobserved, and another for active burrows, with a ‘1’ recorded if an active desert tortoise burrow was observed during the survey and a ‘0’ if one wasn’t observed. Field crews also recorded air temperature (°C) for inclusion as a predictor on daily detection probabilities. We hypothesized that detection probability would decrease as air temperature increased due to desert tortoises avoiding being above ground.

Figure 2. Location of the Boulder City Conservation Easement and occupancy sample plots in Clark County, Nevada, USA. Plots are symbolized by whether a live desert tortoise or active burrow were ever recorded at the plot from 2013 – 2017. Only plots included in the statistical analysis are shown.



We used remote-sensing analysis to develop predictor variables that might be expected to be associated with desert tortoise occurrence (Table 1). Predictor variables can be classified into three general types: topographic, edaphic, and vegetative. Topographic features relate to desert tortoise ability to move around on the landscape, the potential for stable burrow construction, and to some extent exposure to predators (e.g., slightly rough landscapes may provide improved hiding cover for desert tortoises). The edaphic predictor variable was included in case it was associated with occurrence via stable burrow construction. The vegetative variables reflect biotic habitat influences, including being a general measure of food availability and shade/cover availability.

Table 1. Types and units of remote-sensed predictor variables assessed in the statistical model for desert tortoise occupancy on the Boulder City Conservation Easement, Clark County, Nevada, USA.

Type of predictor	Predictor variable	Units; notes
Topographic	Distance to road	Euclidean distance (100m) to nearest paved/unpaved road
	Roughness ¹	Root mean square diff in raster cell elevation from neighbor (x10); lower values = smoother area.
	Slope ¹	Percent slope, in tenths of a percent; 100% = 45 degrees.
	Wetness ¹	Unipath wetness index (x10); low values = drier area.
	Washes ¹	Average density of washes (10 m / ha) w/in 25 m of cell.
Edaphic	Dominant soil ¹	Soil Great-Group type
Vegetative	Creosote cover ¹	Areal coverage of creosote (sq. decimeters / 25 m ²)
	Bursage cover ¹	Areal coverage of bursage (sq. decimeters / 25 m ²)

¹These variables calculated by University of Texas at Austin. See Young et al. (2017) for details on variable calculation. Most variables were transformed from Young et al. (2017) to facilitate model convergence and interpretation of the intercept.

All remote-sensed predictor variables were initially generated on a 5m x 5m raster grid (see Young et al. 2017 for detailed discussion of variable creation). All variables were resampled as the average of all grid cells within the 4 ha occupancy sampling plots. Several topographic and vegetative variables were also calculated at the 40 ha scale, but average values for each variable at this larger scale were highly correlated with the average values at the 4 ha scale ($r > 0.9$). Only the 4 ha plot-level predictor variables were used in the analysis. The available vegetative variables also included total vegetative areal coverage and volume estimates for creosote (*Larrea tridentate*), bursage (*Ambrosia dumosa*), and total vegetation. Only areal coverage of creosote and bursage were used in the analysis because total vegetation area was highly correlated with bursage cover ($r = 0.89$), bursage and creosote cover were only weakly correlated with each other ($r = -0.27$), and volume measurements for all variables were a linear calculation based on the remote-sensed areal estimates (Young et al. 2017). For creation of the predictive raster surface using results of the statistical model, the predictor variable rasters were reclassified using a neighborhood analysis in GIS, such that each grid cell represented the mean

value for that predictor within a 4 ha square centered on the grid cell. This way the calculation of the predictive surface was equivalent to that of the input data in the statistical model. Some variables were adjusted (e.g., divide all values by 100) from Young et al. (2017) to improve statistical model convergence and to facilitate a natural interpretation of the intercept values in the model. All variables were centered (i.e., mean subtracted from observed) to facilitate analysis. Possible quadratic forms for all variables were investigated prior to specification of the final model. The predictive surface based on the final model was created using the Raster Calculator tool. All spatial analysis was done in ArcGIS 10.4.1.

Statistical model

I built a Bayesian state-space hierarchical occupancy model (Panel 1; sensu Royle & Kerry 2007, Nichols et al. 2008, and Mordecai et al. 2011). Each site i had an underlying true occupancy state ($\psi[i]$) that was observed via a random permutation of apparent yearly occupancy ($z[i,j]$ for site i and year j), conditional on true occupancy. The within-year survey data fed into each site's apparent yearly occupancy. Statistical analyses were completed using 'r2jags' and 'coda' in R 3.4.0.

Model and predictive surface validation

It is important to ensure three things about a statistical model's output, especially one as complex as this one. First, we need to verify the internal integrity of the Bayesian model performance to determine if the output is reliable (conditional on the model structure and input). Second, we need to determine if the predictive surface is supported by our input data to ensure no statistical problems or raster GIS problems in the process from raw data to model output to predictive surface. Third, when sufficient independent data exist, it is very useful to evaluate the accuracy of the predictive surface by comparing it to independent data.

Here, we had access to all three levels of validation. First, model performance was assessed internally through inspection of Markov Chain Monte Carlo (MCMC) plots and R-hat diagnostics. Second, alignment of the predictive surface with the input data was achieved via logistic regression whether an occupancy sampling plot ever had a live tortoise or active burrow detection against the mean predictive surface value within the plot. Third, I used desert tortoise telemetry locations in the northern half of the BCCE and correlation analyses to determine if resident tortoises used the BCCE proportional to what is predicted in the occupancy predictive surface. Together, these three validation methods provide a strong assessment of the accuracy and robustness of the model results and the predictive occupancy surface.

Panel 1. Bayesian state-space hierarchical model for desert tortoise occupancy in the Boulder City Conservation Easement, Clark County, Nevada, USA, 2013 – 2017. This is the model specification in the JAGS language. See Appendix A for full R code to replicate the analysis.

```
#Priors for hyperparameters
b.di strd~dnorm(0, 0.0001)
b.di strd.quad~dnorm(0, 0.0001)
b.rough~dnorm(0, 0.0001)
b.rough.quad~dnorm(0, 0.0001)
b.slope~dnorm(0, 0.0001)
b.veg.t1~dnorm(0, 0.0001)
b.veg.t2~dnorm(0, 0.0001)
b.ptemp~dnorm(0, 0.0001)

pao <- sum(psi [])      #derived number of sites occupied

#Estimates of year-specific probabilities of detection
for(j in 1:nYears){
  p.vis.year[j] ~ duni f(0, 1)
  p.burr.year[j] ~ duni f(0, 1)
  z.year[j] <- sum(z[,j])
  yr.apparent[j] ~ duni f(0, 1) } #end nYears loop

#yearly apparent occupancy observation equation
for(i in 1:nSite){
  #State model
  psi0[i]~dnorm(0, 0.0001)
  psi.logit[i] <- psi0[i] + b.di strd*di stroad[i]+b.di strd.quad*di stroad[i]*d
    i stroad[i] + b.rough*rough[i] + b.rough.quad*rough[i]*rough[i] +
    b.slope*slope[i] + b.veg.t1*veg.t1[i] + b.veg.t2*veg.t2[i]
  psi[i] <- exp(psi.logit[i])/(1+exp(psi.logit[i]))

  # Observation model
  for(j in 1:nYears){
    z[i,j] ~ dbern(psi[i]*yr.apparent[j])

    for(k in 1:nSurveys){
      yvis[i,k,j] ~ dbern(detprob.vis[i,k,j]*z[i,j])
      yburr[i,k,j] ~ dbern(p.burr.year[j]*z[i,j])
      detprob.vis.logit[i,k,j] <- p.vis.year[j] + b.ptemp*ptemp[i,k,j]
      detprob.vis[i,k,j] <- exp(detprob.vis.logit[i,k,j])/(1+exp(detprob.v
        is.logit[i,k,j]))
      ptemp[i,k,j]~dnorm(0, 0.0001)
    }
  }
}
```

Results

Occupancy surveys were conducted from early to late April in 2013 and 2014 and from early April to mid-June in 2015, 2016, and 2017. All surveys were conducted at least one week apart at each plot. The order of plots surveyed was randomized each survey. In total there were 1,710 plot surveys conducted that were used in this analysis.

There were a total of 96 live tortoise detections across all sites and years, with 10, 6, 22, 22, and 36 observations in years 2013 through 2017, respectively. There were a total of 63

active burrow detections, with 12, 5, 8, 9, and 29 in years 2013 through 2017, respectively. Mean distance to road across the plots was 1,020.1 m (SD 878.0), mean roughness index was 0.73 (SD 0.36), mean slope was 2.74% (SD 1.1), mean areal coverage of creosote was 0.56 m² per 25m² (SD 0.31), mean coverage of bursage was 2.47 m² per 25m² (SD 0.66), mean wetness index was -5.37 (SD 0.79), and mean wash density was 0.011 m/ha (SD 0.008). There were four dominant soil types: Haplargids, Haplocalcids, Torriorthents, and Torripsamments. The proportion of sites that ever had a detection of a live tortoise or active burrow was higher for sites in Haplocalcid soils (56.0% had detections) and Torriorthent soils (54.3%) than at sites in Haplargid soils (21.4%) and Torripsamment soils (0.00%; only a single site in this soil type).

Conditional density plots were examined for all variables to determine if any variables might exhibit a quadratic relationship with occupancy. This identified that the variables distance to road, roughness, slope, and wash density potentially had quadratic relationships and quadratic terms were included in the saturated model. A saturated model (i.e., all possible predictor variables, including quadratic terms where possible) was then built to identify meaningful variables for the final model. After inspection of the posterior densities, the variables quadratic slope, wetness, and wash density were removed from further consideration because the posterior densities for the associated coefficients broadly overlapped zero. Dominant soil type was initially included, but in the final model it resulted in extreme logit values that distorted the coefficient estimates of the other variables. Dominant soil was removed from the final model to obtain reasonable parameter estimates of the other variables. The final statistical model for occupancy was:

$$\text{logit}(\psi_i) = \psi 0_i + \beta_{\text{distrd}} * \text{Distrd}_i + \beta_{\text{distrd}2} * \text{Distrd}_i^2 + \beta_{\text{rough}} * \text{Rough}_i + \beta_{\text{rough}2} * \text{Rough}_i^2 + \beta_{\text{slope}} * \text{Slope}_i + \beta_{\text{veg.t1}} * \text{Veg.t1}_i + \beta_{\text{veg.t2}} * \text{Veg.t2}_i$$

where ψ_i is the true occupancy of site i , $\psi 0_i$ is an intercept occupancy value in the absence of covariates, β_x is the coefficient estimate for predictor variable x , veg.t1 is creosote cover, and veg.t2 is bursage cover. Survey-level detection probability for active tortoises had a single predictor variable that adjusted the year-specific detection probability estimate:

$$\text{logit}(p_j) = p.\text{year}_j + \beta_{\text{temp}} * \text{Temp}_{ijk}$$

where p_j is the detection probability for live tortoises in year j conditional on an intercept for detection probability in year j ($p.\text{year}_j$) and the air temperature during the survey at site i in year j on survey k .

After removing the non-meaningful variables and withholding the dominant soil type variable the final model was run to obtain coefficient estimates and posterior density distributions for the statistical model. The final model was run for 100,000 MCMC iterations on three separate chains. The first 10,000 iterations were discarded for burn-in and the remaining iterations were thinned to every 30th draw to reduce autocorrelation in the posterior draws, resulting in 9,000 iterations saved for inference.

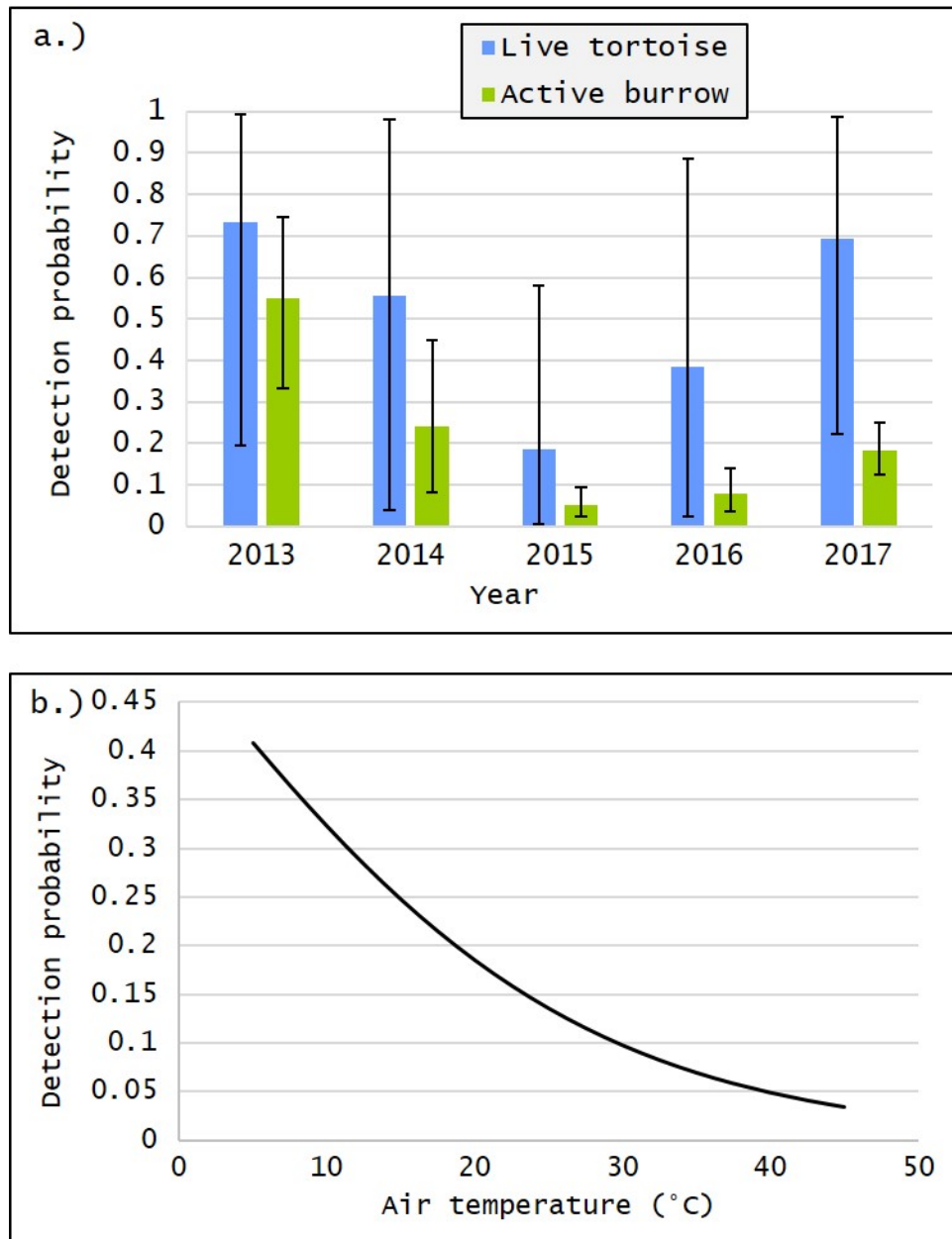
The final model found several important relationships between site occupancy and landscape variables. A site was more likely to be occupied the further it was from a road ($\beta_{\text{road}} =$

5.73, 95% Cr.I = -1.16, 12.52). The positive linear term and a significant positive quadratic term ($\beta_{\text{road}2} = 0.96$, 95% Cr.I = 0.18, 1.56) for distance to road meant that the probability of occupancy increased non-monotonically, such that the rate of increasing likelihood of occupancy increased with distance from a road. Sites were more likely to be occupied at low levels of topographic roughness, and likelihood of non-occupancy increased rapidly as roughness increased ($\beta_{\text{rough}} = -3.84$, 95% Cr.I = -37.24, 28.98; $\beta_{\text{rough}2} = -3.71$, 95% Cr.I = -8.17, -0.21). Although the variable 'slope' was retained in the final model, the 95% Credible Interval of the coefficient estimate broadly overlapped zero and was therefore not significant or meaningful ($\beta_{\text{slope}} = 5.617$, 95% Cr.I = -5.03, 16.91). Creosote coverage was non-significantly negatively related to occupancy, meaning that occupancy of sites tended to decline as creosote coverage on the plot increased ($\beta_{\text{veg.t1}} = -0.92$, 95% Cr.I = -3.00, 1.02). Bursage coverage was significantly related to occupancy, with increasing coverage of bursage associated with increasing rates of site occupancy ($\beta_{\text{veg.t2}} = 0.89$, 95% Cr.I = 0.15, 1.66). The bursage coverage coefficient can be exponentiated, giving an odds ratio on occupancy as a function of unit changes in bursage cover. A site was 2.44 (95% Cr.I = 1.15, 5.23) times more likely to be occupied with every 1 decimeter²/25m² increase in bursage cover.

Parameters for probability of detection showed considerable variation among years. The probability of detecting a live tortoise in a single survey, given the site was truly occupied, ranged from 0.185 in 2015 to 0.734 in 2013. The probability of detecting an active burrow, given occupancy, ranged from 0.530 in 2015 to 0.549 in 2013 (Figure 3a). In addition to the year-specific visual detection probability, the probability of detecting a live tortoise decreased as air temperature increased ($\beta_{\text{temp}} = -0.074$, 95% Cr.I. = -0.087, -0.060). Exponentiating the temperature coefficient indicates that for every 1.0 °C increase in air temperature, the probability of detecting a live tortoise at an occupied site decreases 7.1%. With a 10°C increase in air temperature there is a 52.3% decrease in the odds of detecting a live tortoise (Figure 3b).

The underlying state variable of interest, true occupancy status, was predicted for each site based on the survey results from all five years and the influence of the landscape predictors on the inherent likelihood of that site's occupancy by desert tortoise (Appendix C). As expected, sites that ever had a live tortoise or active burrow detected on them in any survey were predicted to be occupied (i.e., the frequency of desert tortoise encounters over the survey period ≈ 1.0). All of the sites that never had a tortoise or burrow detection had variable probabilities of true occupancy (i.e., predicted frequencies of tortoise encounters). The probabilities for these sites ranged from 0.00 to 0.99, with the majority being below 0.10. The variation in these values is due to the influence of the landscape predictors, which for a handful of sites strongly indicated that they likely have high expected frequency of occurrence, but by chance both tortoises and active burrows happened to go undetected in all five years. Most remaining sites were predicted to have low (≈ 0.20) or very low (≈ 0.01) frequencies of encounters with desert tortoise.

Figure 3. Year-specific and temperature-influenced detection probabilities for live desert tortoises and active burrows at occupied sites in the Boulder City Conservation Easement, Clark County, Nevada, USA, 2013 – 2017. Error bars are 95% credible intervals.



In addition to the true underlying occupancy state, the model included a term for “apparent annual occupancy”, which directly estimated the process by which some sites that were truly occupied did not have any detections in some years. The proportion of truly occupied sites that appeared occupied in any given year was 0.19, 0.20, 0.66, 0.49, and 0.63 consecutively in years 2013 through 2017. This highlights that many of the sites that were truly occupied had years where that occupancy went undetected, although this proportion decreased dramatically in

2015 when survey effort increased dramatically (i.e., the yearly apparent occupancy increased dramatically when the number of surveys per year increased from three to seven). The related metric in the model, z_j , which sums the apparent probability of occupancy across all sites in each year, can be used to directly test the assumption of constant occupancy across years. Here, the summed probability of occupancy was 7.29, 7.95, 28.61, 21.00, and 27.23 consecutively in years 2013 through 2017. Again, this directly shows that survey effort affects the proportion of sites that appear occupied. A linear regression on yearly apparent occupancy, after accounting for the different survey effort in 2013-2014 versus 2015-2017, found that there was no trend in yearly apparent occupancy ($p = 0.885$). Combined with knowledge on desert tortoise ecology and life history, this supports the validity of the assumption of constant true occupancy within this time frame.

The predictor variable coefficients were inserted into the statistical model above and then applied to the input raster layers for each predictor variable, creating a continuous predictive surface of relative frequency of occurrence of desert tortoise across the BCCE (Figure 4). The predictive surface was originally a distribution of index values on the logit scale, which were reclassified into equal-area bins, ranging from '1' (the lowest predicted frequency of occurrence), to '5' (the highest predicted frequency of occurrence). In other words, an equal proportion of the BCCE occurs in each predicted frequency bin, and the bins occur in rank order. Note that the map does not represent predicted presence and absence of desert tortoise, only relative frequency of occurrence.

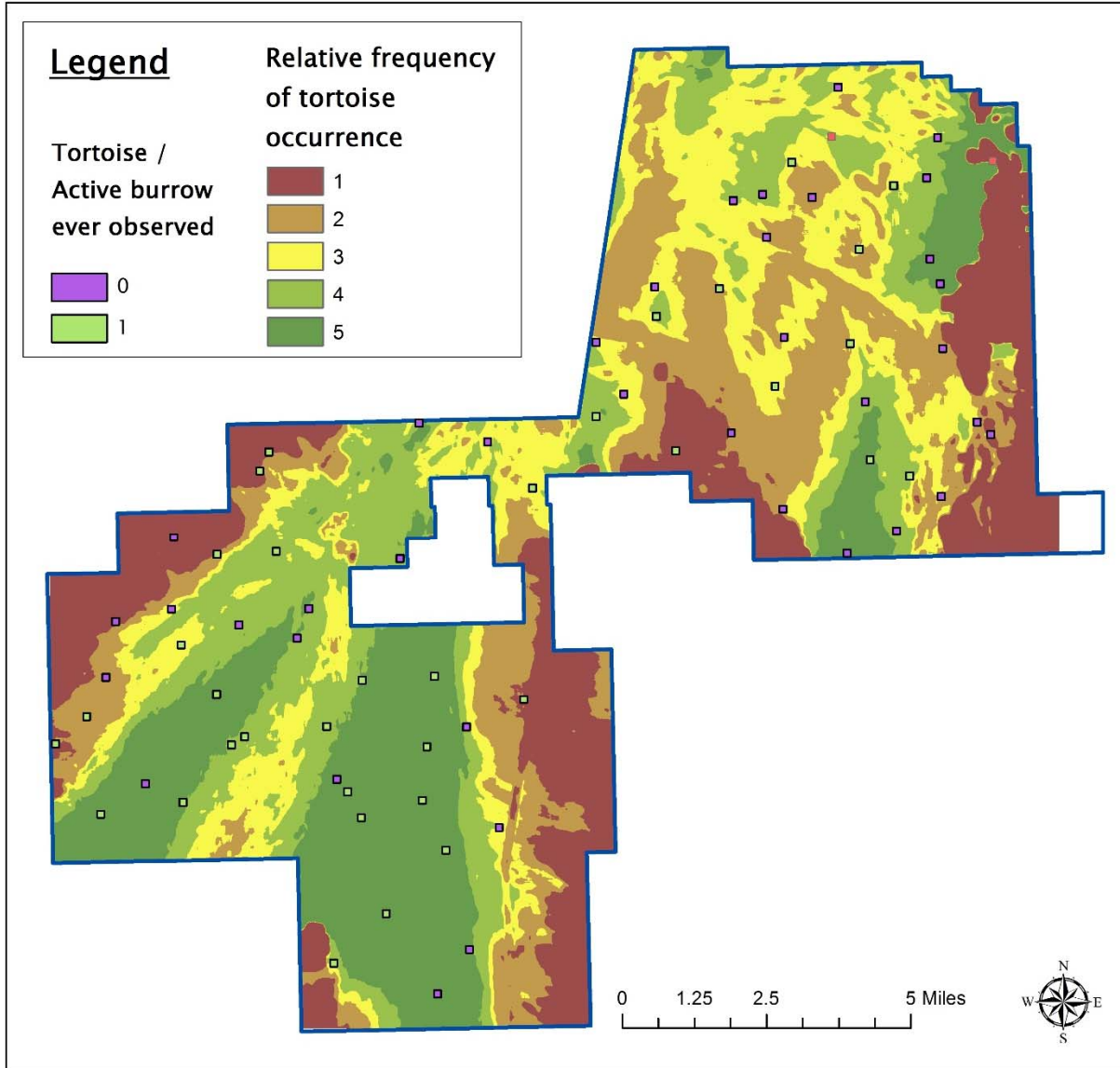
Validation

The statistical model and predictive raster surface were validated in three ways: internal MCMC sampler diagnostics, how well the raster surface predicted the input desert tortoise survey data, and how well the raster surface predicted the space use of independent radio-telemetered desert tortoises.

First, the MCMC sampler diagnostics showed solid and reliable performance of the MCMC sampler and resultant inference on specific parameters. All three chains converged on the same distributions for parameters, including deviance, and showed a high degree of mixing. For most monitored parameters, including deviance, there was low autocorrelation in the sample draws. R-hat indices, a measure of the mixing ratios of each parameter's posterior distribution across the three chains, were below 1.05 for all but three of the 103 monitored parameters, often below 1.002. This indicates reliable inference can be made on the posterior distributions of the parameters of interest (conditional on model structure and input data).

Second, the detection history at sample sites was well predicted by the underlying predictive raster surface. Logistic regression found that as the mean predicted frequency of occurrence within the site increased, the site was more likely to have ever had a detection of a live tortoise or active burrow ($\beta_{\text{mean}} = 0.518$, 95% C.I. = 0.127, 0.909; $p = 0.009$). This indicates a statistically-significant relationship whereby the predictive surface was related positively to the frequency of desert tortoise occurrences.

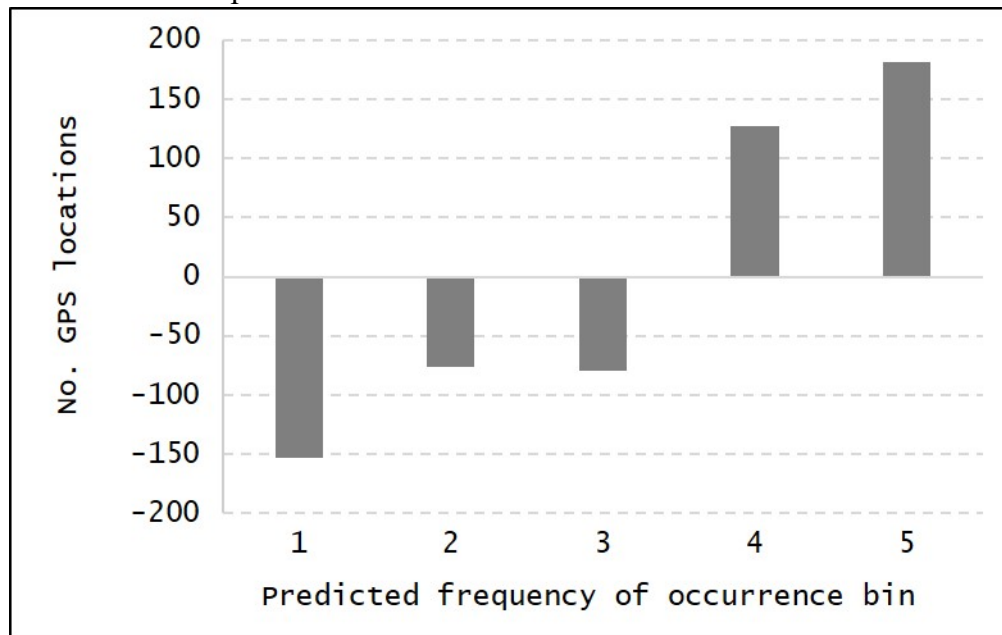
Figure 4. Predicted relative frequency of occurrence of desert tortoise across the Boulder City Conservation Easement, Clark County, Nevada, USA, 2013-2017. Predicted frequency of occurrence was reclassified into five equal-area bins ranging from ‘1’ (lowest frequency) to ‘5’ (highest frequency).



Third, GPS locations from independent radio-telemetered desert tortoises were plotted on top of the predictive raster surface. These locations were only in the northern portion of the BCCE. The predicted frequency bin for the grid cell under the location was sampled, and the frequency of locations occurring in each bin was compared to the expected occurrence at random given the spatial composition of all predictive frequency bins across the north BCCE (i.e., if the predictive surface was unrelated to how desert tortoise use the landscape, the frequency of GPS locations would be random with respect to the bins of the predictive surface). The correlation analysis found that there was a significant linear relationship, whereby desert tortoises occurred

in the predicted low frequency portions of the BCCE less often than expected and occurred in the high predicted frequency portions more often than expected (Pearson's $r = 0.948$, $p = 0.014$). This analysis demonstrated that the predictive raster surface performed very well at predicting the spatial variation in occurrence of independent desert tortoises in the BCCE. Note that the lower frequency bins do not indicate "non-habitat", as 117 of the GPS locations did occur in predicted frequency bin '1'. Rather, this highlights the strong performance of the raster surface as a predictor of relative frequency of occurrence.

Figure 5. Number of independent desert tortoise GPS locations in each predicted frequency of occurrence bin in the Boulder City Conservation Easement, Clark County, Nevada, USA. Number is compared to the number expected if GPS locations were random with respect to the predicted frequency raster surface (i.e., 150 fewer GPS locations occurred in the lowest predicted frequency bin than expected at random). This analysis shows that independent tortoises used the lowest predicted frequency far less than expected and the highest predicted frequency areas far more than expected, indicating that the predictive raster surface did well at predicting the habitat use and occurrence of independent desert tortoises.



Conclusion

The novel Bayesian state-space hierarchical occupancy model performed well and achieved the goals of the project. It leveraged the full sampling dataset and provided a single estimate of the relationships between landscape variables and the frequency of encounters of desert tortoise in the BCCE. Desert tortoise were more likely to occur in areas far from roads, with low topographic roughness, with low areal coverage of creosote, and with high areal coverage of bursage. The probability of detecting a live desert tortoise or active burrow during a single survey, if the site was truly occupied, was highly variable among years. Detectability of live tortoises was also strongly dependent on air temperature at the time of the survey, with

detectability decreasing as air temperature increased. The statistical model validated well internally, and did very well at predicting the survey history of sample sites and the habitat use of independent desert tortoises.

The calculation of yearly apparent occupancy is the crux of evaluating the assumption of constant occupancy within the time period analyzed. Standard occupancy models assume constancy within years and dynamic models explicitly model change in true occupancy among years. The state-space model presented here rests on the assumption of constant occupancy across the years analyzed (or, if modified, could allow for explicit testing of trends in occupancy). A post-hoc analysis of the proportion of the sites that appeared occupied in each year did not support rejection of this assumption, as there was no trend in apparent occupancy after adjusting for survey effort. A clear caveat to this assumption is that at some length of time the assumption is no longer tenable. Even a long-lived low-recruitment species like desert tortoise will eventually show changes in the proportion of area that is occupied, particularly in the face of dramatic population declines.

The failure to reject the assumption of constant occupancy here has clear implications for using occupancy monitoring as a tool to monitor desert tortoise populations. First, making this assumption was only necessary in order to model single relationships between landscape predictor variables and true occupancy in the presence of high annual variability in detectability of desert tortoise. It is not inherent that this assumption be made for an occupancy monitoring program, and indeed, this state-space model could be modified to directly test for temporal trends in occupancy subject to high annual variability in detectability. Second, it is reasonable to make the assumption of constant occupancy, over (relatively) short time periods, given desert tortoise ecology and life history. The proportion of desert tortoise habitat that is occupied cannot increase dramatically in a short period of time, but can decrease rapidly. We did not see evidence of a rapid decline in this data set, probably at least partially due to the protected conservation status of the BCCE. Occupancy monitoring has been demonstrated to be more efficient and powerful than line-distance sampling (Zylstra et al. 2010). Therefore the most logical step for monitoring is to leverage occupancy sampling as a monitoring tool, but to modify a unified state-space model such as presented here to explicitly test for temporal trends in true occupancy while explicitly accounting for the strong inter-annual variation in detectability and apparent occupancy. Including climatic predictor variables on the apparent occupancy level of this model would be a promising way to adjust for apparent occupancy to better estimate true underlying occupancy in each year. The model presented here is a useful and promising tool for monitoring desert tortoise occupancy trends over time given high annual variability in apparent occupancy.

Literature cited

- Bailey, L.L., D.I. MacKenzie, and J.D. Nichols. (2014) Advances and applications of occupancy models. *Methods in Ecology and Evolution* 5:1269-1279.
- Desert Conservation Program. (2011) Monitoring protocol: Testing the use of occupancy sampling to detect status and trends of Mojave desert tortoise (*Gopherus agassizii*) in the

Boulder City Conservation Easement. Clark Country Multiple Species Habitat Conservation Plan, Desert Conservation Program. Prepared by Enduring Conservation Outcomes. Revised 2013.

- Duda, J.J., A.J. Krzysik, and J.E. Freilich. (1999) Effects of drought on desert tortoise movement and activity. *Journal of Wildlife Management* 63:1181-1192.
- Franks, B.R., H.W. Avery, and J.R. Spotila. (2011) Home range and movement of desert tortoises *Gopherus agassizii* in the Mojave Desert of California, USA. *Endangered Species Research* 13:191-201.
- Graves, T.A., J.A. Royle, K.C. Kendall, P. Beier, J.B. Stetz, A.C. Macleod. (2012) Balancing precision and risk: should multiple detection methods be analyzed separately in N-mixture models? *PLoS One* 7:e49410.
- MacKenzie, D.I., J.D. Nichols, G.B. Lachman, S. Droege, J.A. Royle, and C.A. Langtimm. (2002) Estimating site occupancy rates when detection probabilities are less than one. *Ecology* 83:2248-2255.
- Mordecai, R.S., B.J. Mattsson, C.J. Tzilkowski, and R.J. Cooper. (2011) Addressing challenges when studying mobile or episodic species: hierarchical Bayes estimation of occupancy and use. *Journal of Applied Ecology* 48:56-66.
- Nichols, J.D., L.L. Bailey, A.F. O'Connell Jr., N.W. Talancy, E.H.C. Grant, A.T. Gilbert, E.M. Annand, T.P. Husband, and J.E. Hines. (2008) Multi-scale occupancy estimation and modelling using multiple detection methods. *Journal of Applied Ecology* 45:1321-1329.
- Royle, J.A., and M. Kéry. (2007) A Bayesian state-space formulation of dynamic occupancy models. *Ecology* 88:1813-1823.
- Young, M.H., J.H. Andrews, T.G. Caldwell, and K. Saylam. (2017) Airborne LiDAR and aerial imagery to assess potential burrow locations for the desert tortoise (*Gopherus agassizii*). *Remote Sensing* 9:458.
- Zylstra, E.R., R.J. Steidl, and D.E. Swann. (2010) Evaluating survey methods for monitoring a rare vertebrate, the Sonoran desert tortoise. *Journal of Wildlife Management* 74:1311-1318.

Appendix A: JAGS model code for the dual-method multiple-season occupancy model to estimate environmental relationships underlying occupancy in the presence of high annual variability in apparent occupancy.

Statistical code for building and running a dual-method multiple-season occupancy model in JAGS using R as an # interface. Code is written to be replicated via copy-paste after changing the input file path to reflect where # the input .csv is stored on the user's computer. Annotation comments follow a hashtag (#) and are ignored by # R.

```
library(R2jags)
library(coda)
```

```
dt.full.data <- read.csv("C:/Users/Heron Ecological/Documents/HeronEcological/Clark
County_NV/ScienceAdvisorPanel/OccupancyAnalyses/Data/occu_jags_fullcovar_centered_R
input.csv", header=TRUE, colClasses = c("factor", rep("numeric", 71), "factor", rep("n
umeric", 20)))
#str(dt.full.data) #a check that data was imported and attributed correctly
```

```
dt.surveytemp.data <- read.csv("C:/Users/Heron Ecological/Documents/HeronEcological
/ClarkCounty_NV/ScienceAdvisorPanel/OccupancyAnalyses/Data/survey_temps.csv", heade
r=TRUE, colClasses=c(rep("numeric", 36))) #read in the survey-level predictor
```

```
dt.full.vis <- dt.full.data[, 2:36] #isolate visual-detection response data
dt.full.burr <- dt.full.data[, 37:71] #isolate burrow-detection response data
dt.covar.temp <- dt.surveytemp.data[, 2:36]
```

```
nSite <- 75 #Specify constants for model looping
nSurveys <- 7
nYears <- 5
```

```
#create arrays of multi-dimensional data
dt.vissarray <- array(as.matrix(dt.full.vis), dim=c(nSite, nSurveys, nYears))
#print(dt.array) #internal check; yep, looks good
dt.burrarray <- array(as.matrix(dt.full.burr), dim=c(nSite, nSurveys, nYears))
dt.temparray <- array(as.matrix(dt.covar.temp), dim=c(nSite, nSurveys, nYears))
```

```
#data transformation on already-centered variables to improve
#model convergence and get sensible intercept estimates
dt.full.data$dist.road.c2 <- dt.full.data$dist.road.c/100
dt.full.data$rough.c2 <- dt.full.data$rough.c*10
dt.full.data$slope.c2 <- dt.full.data$slope.c*10
dt.full.data$veg.area.t1.c2 <- dt.full.data$veg.area.t1.c*100
dt.full.data$veg.area.t2.c2 <- dt.full.data$veg.area.t2.c*100
dt.full.data$wetness.c2 <- dt.full.data$wetness.c*10
dt.full.data$wash25m.ha.c2 <- (dt.full.data$wash25m.ha.c)/10
```

```
#list data to be included/accessed during the model run
jags.final.rescaled.data <- list(yvis = dt.vissarray, yburr = dt.burrarray, distroad
=dt.full.data$dist.road.c2, rough=dt.full.data$rough.c2, slope=dt.full.data$slope.c
2, veg.t1=dt.full.data$veg.area.t1.c2, veg.t2=dt.full.data$veg.area.t2.c2, ptemp=dt.
temparray, nSite = nSite, nYears = nYears, nSurveys = nSurveys)
```

```
#JAGS needs starting values that are close to observed values, pull from data
z.init <- apply(dt.full.data[, 2:71], 1, max, na.rm=TRUE) #ignore NA's
z.init <- cbind(z.init, z.init, z.init, z.init, z.init) #Year init values
```

Full JAGS model statement

```
jags.final.model <- function(){  
  
  #Priors for hyperparameters  
  b.di.strd~dnorm(0, 0.0001)  
  b.di.strd.quad~dnorm(0, 0.0001)  
  b.rough~dnorm(0, 0.0001)  
  b.rough.quad~dnorm(0, 0.0001)  
  b.sl.ope~dnorm(0, 0.0001)  
  b.veg.t1~dnorm(0, 0.0001)  
  b.veg.t2~dnorm(0, 0.0001)  
  b.ptemp~dnorm(0, 0.0001)  
  
  #Derived quantities of interest  
  pao <- sum(psi []) #derived number of sites occupied  
  
  #Estimates of year-specific probabilities of detection  
  for(j in 1:nYears){  
    p.vis.year.logit[j] ~ dnorm(0, 0.0001)  
    p.burr.year[j] ~ duniform(0, 1)  
    p.vis.year[j] <- exp(p.vis.year.logit[j])/(1+exp(p.vis.year.logit[j]))  
    #detprob.burr[j] <- exp(p.burr.year[j])/(1+exp(p.burr.year[j]))  
    z.year[j] <- sum(z[,j])  
    yr.apparent[j] ~ duniform(0, 1)  
  } #end nYears loop  
  
  #yearly apparent occupancy observation equation  
  for(i in 1:nSite){  
    #State model  
    psi0[i]~dnorm(0, 0.0001)  
    psi.logit[i] <- psi0[i] + b.di.strd*di.stroad[i]+b.di.strd.quad*di.stroad[i]*di  
stroad[i] + b.rough*rough[i] + b.rough.quad*rough[i]*rough[i] + b.sl.ope*sl.ope[i] +  
b.veg.t1*veg.t1[i] + b.veg.t2*veg.t2[i]  
    psi[i] <- exp(psi.logit[i])/(1+exp(psi.logit[i]))  
  
    # Observation model  
    for(j in 1:nYears){  
      z[i,j] ~ dbern(psi[i]*yr.apparent[j])  
  
      for(k in 1:nSurveys){  
        yvis[i,k,j] ~ dbern(detprob.vis[i,k,j]*z[i,j])  
        yburr[i,k,j] ~ dbern(p.burr.year[j]*z[i,j])  
        detprob.vis.logit[i,k,j] <- p.vis.year.logit[j] + b.ptemp*ptemp[i,k  
,j]  
        detprob.vis[i,k,j] <- exp(detprob.vis.logit[i,k,j])/(1+exp(detprob.  
vis.logit[i,k,j]))  
        ptemp[i,k,j]~dnorm(0, 0.0001)  
      } # end nSurveys loop  
    } #end nYears loop  
  } #end nSite loop  
} #close model specification
```

Tell JAGS what model nodes to monitor and report in output

```
jags.final.params <- c("yr.apparent", "psi", "z.year", "pao", "b.distrd", "b.distrd.quad", "b.slope", "b.veg.t1", "b.rough", "b.rough.quad", "b.veg.t2", "b.ptemp", "p.vis.year", "p.burr.year")
```

```
# Give JAGS initial starting values for the gnarlier stochastic nodes
```

```
jags.inits <- function(){list("p.vis.year.logit" = rnorm(5), "p.burr.year" = runif(5), "z" = z.init)}
```

```
# Execute JAGS model
```

```
# 100k draws from posterior distribution, discard first 10k draws for burn-in
```

```
# thin to every 30th draw to reduce serial autocorrelation in posterior draws
```

```
# ran these parameters on three parallel chains to assess proper convergence
```

```
dt.final.nosol.jagsfit <- jags(data=jags.final.rescaled.data, parameters.to.save=jags.final.params, inits=jags.inits, n.iter=100000, n.burnin=10000, n.thin=30, model.file=jags.final.model)
```

```
#call the results
```

```
dt.final.nosol.jagsfit
```

Appendix B. Full model results from monitored nodes in the JAGS dual-method multi-year occupancy model outlined in Appendix A. ‘pao’ is the estimated proportion of samples sites that are occupied, and ‘psi[i]’ is the predicted probability of true occupancy for site [i]. ‘Deviance’ is the distance of the current model from a fully-saturated model (i.e., it is unit-less and intended for comparison among models). ‘Mu.vect’ is the average value from the conditional posterior density surface and can be interpreted as the ‘best estimate’. The 2.5% through 97.5% quantiles are the parameter values associated with the stated quantile value of the posterior density surface. The 2.5 and 97.5% are similar to the bounds of a 95% confidence interval, except in this Bayesian model they represent true probability bounds (e.g., there is a 95% probability that the true detection probability for active burrows in 2013 [p.burr.year[1]], given desert tortoise presence, is between 0.332 and 0.745). Rhat is a measure of parameter convergence and should be < 1.10. N.eff is the effective number of samples contributing to the posterior density. Note that because this is a stochastic Bayesian model, if the code in Appendix A is run it will yield slightly different estimates than presented here.

	mu.vect	sd.vect	2.5%	25%	50%	75%	97.5%	Rhat	n.eff
b.di.strd	5.730	3.520	-1.155	3.379	5.734	8.090	12.523	1.001	9000
b.di.strd.quad	0.957	0.349	0.178	0.745	0.992	1.201	1.560	1.001	7400
b.ptemp	-0.074	0.007	-0.087	-0.078	-0.074	-0.069	-0.060	1.001	9000
b.rough	-3.838	16.902	-37.242	-15.362	-3.706	7.465	28.980	1.004	560
b.rough.quad	-3.709	2.093	-8.167	-5.070	-3.539	-2.178	-0.205	1.002	1800
b.slope	5.617	5.616	-5.034	1.724	5.505	9.423	16.907	1.007	360
b.veg.t1	-0.920	1.044	-2.998	-1.620	-0.883	-0.196	1.024	1.003	1000
b.veg.t2	0.892	0.382	0.146	0.630	0.883	1.145	1.655	1.001	4800
p.burr.year[1]	0.549	0.107	0.332	0.477	0.552	0.625	0.745	1.001	9000
p.burr.year[2]	0.241	0.095	0.083	0.171	0.232	0.299	0.450	1.001	9000
p.burr.year[3]	0.053	0.018	0.024	0.040	0.051	0.064	0.096	1.001	9000
p.burr.year[4]	0.080	0.026	0.038	0.061	0.078	0.096	0.139	1.001	5100
p.burr.year[5]	0.184	0.031	0.126	0.162	0.182	0.204	0.249	1.001	9000
p.vi.s.year[1]	0.734	0.216	0.194	0.611	0.788	0.907	0.992	1.001	9000
p.vi.s.year[2]	0.556	0.274	0.041	0.342	0.574	0.790	0.979	1.001	9000
p.vi.s.year[3]	0.185	0.156	0.006	0.065	0.141	0.268	0.579	1.001	9000
p.vi.s.year[4]	0.385	0.235	0.024	0.196	0.362	0.550	0.887	1.001	4500
p.vi.s.year[5]	0.692	0.210	0.222	0.553	0.724	0.864	0.985	1.001	9000
pao	43.116	2.168	39.171	41.696	42.996	44.375	47.890	1.001	9000
psi [1]	0.016	0.122	0.000	0.000	0.000	0.000	0.005	1.002	1200
psi [2]	0.029	0.163	0.000	0.000	0.000	0.000	0.975	1.001	9000
psi [3]	0.256	0.433	0.000	0.000	0.000	0.872	1.000	1.001	8400
psi [4]	0.998	0.020	0.993	1.000	1.000	1.000	1.000	1.036	4500
psi [5]	0.996	0.047	1.000	1.000	1.000	1.000	1.000	1.001	9000
psi [6]	0.002	0.044	0.000	0.000	0.000	0.000	0.000	1.006	420
psi [7]	0.989	0.077	0.888	1.000	1.000	1.000	1.000	1.010	9000
psi [8]	0.098	0.294	0.000	0.000	0.000	0.000	1.000	1.002	1900
psi [9]	0.047	0.206	0.000	0.000	0.000	0.000	1.000	1.001	9000
psi [10]	0.086	0.278	0.000	0.000	0.000	0.000	1.000	1.002	2800
psi [11]	0.014	0.111	0.000	0.000	0.000	0.000	0.002	1.001	9000
psi [12]	0.997	0.029	0.982	1.000	1.000	1.000	1.000	1.025	9000
psi [13]	0.014	0.111	0.000	0.000	0.000	0.000	0.001	1.001	9000
psi [14]	0.010	0.094	0.000	0.000	0.000	0.000	0.000	1.001	7100
psi [15]	0.975	0.124	0.524	1.000	1.000	1.000	1.000	1.003	9000
psi [16]	0.025	0.151	0.000	0.000	0.000	0.000	0.320	1.001	4500
psi [17]	0.991	0.072	0.994	1.000	1.000	1.000	1.000	1.019	9000
psi [18]	0.049	0.211	0.000	0.000	0.000	0.000	1.000	1.001	9000
psi [19]	0.094	0.286	0.000	0.000	0.000	0.000	1.000	1.001	9000
psi [20]	0.967	0.140	0.412	1.000	1.000	1.000	1.000	1.001	9000

psi [21]	0.017	0.127	0.000	0.000	0.000	0.000	0.007	1.001	4500
psi [22]	0.977	0.120	0.576	1.000	1.000	1.000	1.000	1.001	9000
psi [23]	0.101	0.295	0.000	0.000	0.000	0.000	1.000	1.001	5200
psi [24]	0.228	0.414	0.000	0.000	0.000	0.026	1.000	1.001	9000
psi [25]	0.985	0.096	0.866	1.000	1.000	1.000	1.000	1.011	4800
psi [26]	0.036	0.183	0.000	0.000	0.000	0.000	1.000	1.002	2700
psi [27]	0.087	0.280	0.000	0.000	0.000	0.000	1.000	1.001	9000
psi [28]	0.031	0.170	0.000	0.000	0.000	0.000	1.000	1.001	9000
psi [29]	0.678	0.465	0.000	0.000	1.000	1.000	1.000	1.004	1600
psi [30]	0.046	0.204	0.000	0.000	0.000	0.000	1.000	1.001	9000
psi [31]	0.997	0.025	0.994	1.000	1.000	1.000	1.000	1.023	8400
psi [32]	0.971	0.136	0.436	1.000	1.000	1.000	1.000	1.005	9000
psi [33]	0.991	0.076	0.996	1.000	1.000	1.000	1.000	1.006	9000
psi [34]	0.995	0.045	0.972	1.000	1.000	1.000	1.000	1.001	8100
psi [35]	1.000	0.006	1.000	1.000	1.000	1.000	1.000	1.113	9000
psi [36]	0.326	0.466	0.000	0.000	0.000	1.000	1.000	1.001	9000
psi [37]	0.026	0.155	0.000	0.000	0.000	0.000	0.678	1.001	8800
psi [38]	0.026	0.154	0.000	0.000	0.000	0.000	0.537	1.001	9000
psi [39]	0.110	0.311	0.000	0.000	0.000	0.000	1.000	1.002	2100
psi [40]	0.999	0.011	1.000	1.000	1.000	1.000	1.000	1.015	9000
psi [41]	0.953	0.167	0.272	1.000	1.000	1.000	1.000	1.002	9000
psi [42]	0.011	0.104	0.000	0.000	0.000	0.000	0.000	1.001	9000
psi [43]	0.143	0.346	0.000	0.000	0.000	0.000	1.000	1.001	9000
psi [44]	0.057	0.227	0.000	0.000	0.000	0.000	1.000	1.001	9000
psi [45]	0.095	0.288	0.000	0.000	0.000	0.000	1.000	1.001	9000
psi [46]	0.075	0.259	0.000	0.000	0.000	0.000	1.000	1.001	9000
psi [47]	0.040	0.192	0.000	0.000	0.000	0.000	1.000	1.001	3300
psi [48]	0.195	0.394	0.000	0.000	0.000	0.000	1.000	1.001	9000
psi [49]	0.987	0.075	0.823	1.000	1.000	1.000	1.000	1.003	9000
psi [50]	0.065	0.240	0.000	0.000	0.000	0.000	1.000	1.001	3100
psi [51]	0.995	0.044	0.988	1.000	1.000	1.000	1.000	1.022	9000
psi [52]	0.976	0.122	0.552	1.000	1.000	1.000	1.000	1.006	8100
psi [53]	0.972	0.135	0.459	1.000	1.000	1.000	1.000	1.006	9000
psi [54]	0.987	0.076	0.822	1.000	1.000	1.000	1.000	1.006	5200
psi [55]	0.998	0.031	1.000	1.000	1.000	1.000	1.000	1.086	6600
psi [56]	0.969	0.137	0.442	1.000	1.000	1.000	1.000	1.002	9000
psi [57]	0.340	0.471	0.000	0.000	0.000	1.000	1.000	1.002	2100
psi [58]	0.995	0.042	0.983	1.000	1.000	1.000	1.000	1.016	8100
psi [59]	0.994	0.048	0.954	1.000	1.000	1.000	1.000	1.036	6100
psi [60]	0.983	0.102	0.774	1.000	1.000	1.000	1.000	1.029	5100
psi [61]	0.973	0.129	0.481	1.000	1.000	1.000	1.000	1.016	6800
psi [62]	0.807	0.392	0.000	1.000	1.000	1.000	1.000	1.001	9000
psi [63]	0.950	0.217	0.000	1.000	1.000	1.000	1.000	1.002	9000
psi [64]	1.000	0.006	1.000	1.000	1.000	1.000	1.000	1.287	5100
psi [65]	0.986	0.092	0.894	1.000	1.000	1.000	1.000	1.003	9000
psi [66]	1.000	0.014	1.000	1.000	1.000	1.000	1.000	1.198	3100
psi [67]	1.000	0.004	1.000	1.000	1.000	1.000	1.000	1.077	9000
psi [68]	0.941	0.235	0.000	1.000	1.000	1.000	1.000	1.002	4100
psi [69]	1.000	0.001	1.000	1.000	1.000	1.000	1.000	1.248	4300
psi [70]	1.000	0.009	1.000	1.000	1.000	1.000	1.000	1.215	3100
psi [71]	0.985	0.121	1.000	1.000	1.000	1.000	1.000	1.014	5100
psi [72]	0.999	0.016	1.000	1.000	1.000	1.000	1.000	1.009	9000
psi [73]	0.383	0.483	0.000	0.000	0.000	1.000	1.000	1.001	9000
psi [74]	1.000	0.008	1.000	1.000	1.000	1.000	1.000	1.183	3200
psi [75]	0.994	0.063	1.000	1.000	1.000	1.000	1.000	1.050	7200
yr. apparent[1]	0.185	0.060	0.083	0.142	0.179	0.222	0.314	1.001	9000
yr. apparent[2]	0.199	0.074	0.082	0.145	0.190	0.243	0.366	1.001	6000

yr. apparent[3]	0.657	0.111	0.447	0.580	0.654	0.730	0.881	1.001	9000
yr. apparent[4]	0.488	0.099	0.306	0.419	0.485	0.554	0.690	1.001	9000
yr. apparent[5]	0.626	0.086	0.455	0.567	0.626	0.686	0.790	1.001	9000
z. year[1]	7.286	0.588	7.000	7.000	7.000	7.000	9.000	1.001	9000
z. year[2]	7.951	1.995	6.000	7.000	7.000	9.000	13.000	1.001	9000
z. year[3]	28.610	3.931	22.000	26.000	28.000	31.000	38.000	1.001	9000
z. year[4]	21.002	2.945	16.000	19.000	21.000	23.000	28.000	1.001	9000
z. year[5]	27.232	2.115	24.000	26.000	27.000	29.000	32.000	1.001	9000
deviance	19788.390	16.794	19759.214	19776.269	19787.240	19799.355	19824.311	1.001	9000

For each parameter, n.eff is a crude measure of effective sample size, and Rhat is the potential scale reduction factor (at convergence, Rhat=1).

DIC info (using the rule, $pD = \text{var}(\text{deviance})/2$)

$pD = 141.0$ and $DIC = 19929.4$

DIC is an estimate of expected predictive error (lower deviance is better).

Appendix C. Site-specific probability of true occupancy/frequency of occurrence (probability occupied and 95% credible intervals taken from Appendix B).

Plot ID	Ever observed	Probability Occupied	Lower 95% Cr.I	Upper 95% Cr.I.
1	0	0.02	0.00	0.01
2	0	0.03	0.00	0.98
5	0	0.26	0.00	1.00
6	1	1.00	0.99	1.00
8	1	1.00	1.00	1.00
9	0	0.00	0.00	0.00
10	1	0.99	0.89	1.00
11	0	0.10	0.00	1.00
12	0	0.05	0.00	1.00
13	0	0.09	0.00	1.00
15	0	0.01	0.00	0.00
17	1	1.00	0.98	1.00
18	0	0.01	0.00	0.00
19	0	0.01	0.00	0.00
20	1	0.98	0.52	1.00
21	0	0.03	0.00	0.32
22	1	0.99	0.99	1.00
23	0	0.05	0.00	1.00
24	0	0.09	0.00	1.00
25	1	0.97	0.41	1.00
26	0	0.02	0.00	0.01
27	1	0.98	0.58	1.00
28	0	0.10	0.00	1.00
29	0	0.23	0.00	1.00
30	1	0.99	0.87	1.00
31	0	0.04	0.00	1.00
32	0	0.09	0.00	1.00
33	0	0.03	0.00	1.00
34	0	0.68	0.00	1.00
35	0	0.05	0.00	1.00
36	1	1.00	0.99	1.00
37	1	0.97	0.44	1.00
38	1	0.99	1.00	1.00
39	1	1.00	0.97	1.00
40	1	1.00	1.00	1.00
41	0	0.33	0.00	1.00

Plot ID	Ever observed	Probability Occupied	Lower 95% Cr.I	Upper 95% Cr.I.
42	0	0.03	0.00	0.68
43	0	0.03	0.00	0.54
44	0	0.11	0.00	1.00
45	1	1.00	1.00	1.00
46	1	0.95	0.27	1.00
47	0	0.01	0.00	0.00
48	0	0.14	0.00	1.00
49	0	0.06	0.00	1.00
50	0	0.10	0.00	1.00
51	0	0.08	0.00	1.00
52	0	0.04	0.00	1.00
53	0	0.20	0.00	1.00
54	1	0.99	0.82	1.00
55	0	0.07	0.00	1.00
56	1	1.00	0.99	1.00
57	1	0.98	0.55	1.00
58	1	0.97	0.46	1.00
59	1	0.99	0.82	1.00
60	1	1.00	1.00	1.00
61	1	0.97	0.44	1.00
62	0	0.34	0.00	1.00
63	1	1.00	0.98	1.00
64	1	0.99	0.95	1.00
65	1	0.98	0.77	1.00
66	1	0.97	0.48	1.00
67	0	0.81	0.00	1.00
68	0	0.95	0.00	1.00
69	1	1.00	1.00	1.00
70	1	0.99	0.89	1.00
71	1	1.00	1.00	1.00
72	1	1.00	1.00	1.00
73	0	0.94	0.00	1.00
74	1	1.00	1.00	1.00
75	1	1.00	1.00	1.00
76	0	0.99	1.00	1.00
77	1	1.00	1.00	1.00
78	0	0.38	0.00	1.00
79	1	1.00	1.00	1.00
80	1	0.99	1.00	1.00
